Thermal force induced by the presence of a particle near a solidifying interface

L. Hadji*
Mathematics Department, University of Alabama, Tuscaloosa, Alabama 35487-0350
(Received 1 May 2001; revised manuscript received 16 July 2001; published 16 October 2001)

The presence of a foreign particle in the melt, ahead of a solid-liquid interface, leads to the onset of interfacial deformations if the thermal conductivity of the particle, k_p, differs from that of the melt, k_l. In this paper, the influence of the thermal conductivity contrast on the interaction between the solidifying interface and the particle is quantified. We show that the interface distortion gives rise to a thermal force whose expression is given by $F_{\rm th}=2\pi LGa^3(1-\alpha)/(2+\alpha)T_m$, where L is the latent heat of fusion per unit volume, T_m is the melting point, a is the particle's radius, G the thermal gradient in the liquid phase and $\alpha=k_p/k_l$. The derivation makes use of the following assumptions: (i) the particle is small compared to the horizontal extent of the interface, (ii) the particle is placed in the near proximity of the deformable solid-liquid interface, and (iii) the interface is practically immobile in the calculation of the thermal field, i.e., $V\ll k_lG/L$, where V is the interface growth velocity. An order of magnitude analysis shows that the magnitude of the thermal force may be greater than that of the forces that are usually accounted for in studies of particle-interface interaction, namely, the drag force and the force due to the disjoining pressure. The inclusion of the thermal force in the overall force balance is found to modify the value of the growth rate at which equilibrium is attained. The analysis leads to the prediction that the growth rate at equilibrium is increased for particles with a low thermal conductivity and is decreased for particles with a high thermal conductivity. The derivation of the thermal force is preceded by a detailed analysis of the influence of the thermal conductance contrast on the interface profile.

DOI: 10.1103/PhysRevE.64.051502 PACS number(s): 64.70.Dv, 81.30.Fb, 81.05.Ni

I. INTRODUCTION

An understanding of the interaction between a foreign particle and a solidifying interface is important due to its occurrence in numerous natural and practical processes [1–4]. One of the most important industrial application is in casting wherein solid inclusions are mixed with the melt to improve the material properties of the final cast product, as, for instance, in the manufacture of metal matrix composites. The microstructural homogeneity of these composite materials depends on the final distribution of the inclusions which, in turn, depends on the behavior of the particles at the moving solid-liquid interface. Experiments and mathematical models have demonstrated that the moving interface either pushes or engulfes the particles. Although considerable progress has been made in understanding this phenomenon, its quantification in terms of the material and processing parameters is still poorly understood. We refer the reader to Refs. [5–7] for a review of the problem.

The influence of the thermal gradient on the shape of the solid-liquid interface has been investigated theoretically by Chernov, Temkin, and Mel'nikova [8], Pötschke and Rogge [9], Shangguan, Ahuja, and Stefanescu [4], and Kim and Rohatgi [10], and experimentally by Zubko, Lobanov, and Nikonova [11], Stefanescu *et al.* [12], Pang, Stefanescu, and Dhindaw [13], Ahuja, Stefanescu, and Dhindaw [14], and Stefanescu *et al.* [15]. These studies have included the role of the particle's thermal conductivity on the maximum growth rate at which the particles are pushed by the interface. Sasikumar, Ramamohan, and Pai [16] and Casses and Azouni [17] investigated the influence of the thermal effects on the morphology of the interface in the vicinity of a foreign particle. They apply an interface condition that includes the undercooling effects due to curvature, disjoining pressure, and lubrication pressure. On imposing that the interface temperature conforms to the isotherm corresponding to the melting point of the pure substance, a second-order differential equation for the interface shape is derived and solved. However, Sasikumar, Ramamohan, and Pai [16] and Casses and Azouni [17] use a leading order expression for the temperature that does not satisfy the heat equation in the cylindrical geometry and does not even have the proper power of the coordinates z and r as either z or $r\to\infty$. Sasikumar and Ramamohan [18] correct their paper, but unfortunately they do not present an in depth analysis of the front's profile.

In this paper, we study the effect of the thermal conductivity of a particle on the solid-liquid morphology. An approach similar to that used by Casses and Azouni [17] and Sasikumar, Ramamohan, and Pai [16] is followed to derive a boundary-value problem for the interface shape. Our analysis reveals two new results: (i) The gap separation at the origin is determined as a function of other material parameters when the thermal conductivity difference is the sole source for interface deformation, (ii) an expression for a thermal force is derived. This thermal force owes its exitence to the difference in thermal conductivities between the particle and the melt. We show that this force is significant and must be included in any force balance when studying particle-interface interaction.

II. MATHEMATICAL FORMULATION

Consider a spherical particle of radius a and thermal conductivity k_p. As shown in the schematic diagram Fig. 1, the particle is placed in the melt a distance h_∞ from the planar

*Email address: lhadji@euler.math.ua.edu

 ©2001 The American Physical Society

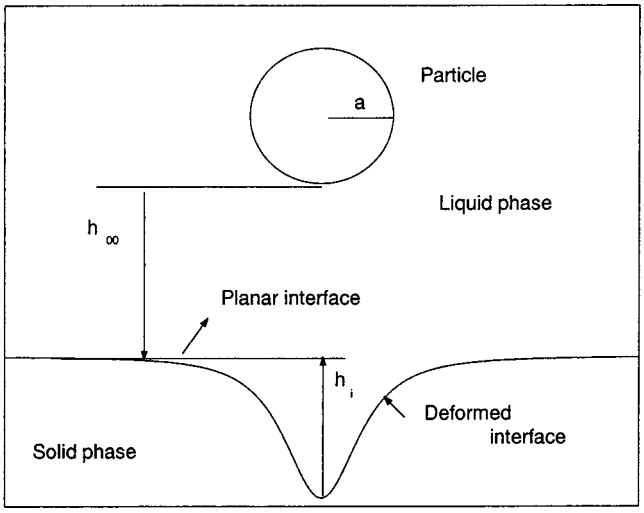

FIG. 1. Sketch of a deformed solid-liquid interface near a particle of radius a; h_∞ is the distance between the lowest point of the particle's surface and the planar interface and h_i is the amount of interfacial distortion at the origin.

solid-liquid interface. We suppose that (i) the particle is neutrally buoyant, (ii) there is no change in heat conductivities upon solidification, and (iii) the interface growth rate is low enough that the solid front-particle system can be considered immobile in the determination of the thermal field. This requires that the interface velocity V satisfies $V \ll k_l G/L$, where k_l is the melt's thermal conductivity, G is the thermal gradient in the melt away from the interface, and L is the latent heat of fusion per unit volume [5].

Under these assumptions, the thermal field induced by the particle-interface interaction is described by the steady state form of the heat conduction equations in the melt and in the particle with the appropriate coupling at the boundaries. On using an axisymmetric geometry with the vertical coordinate denoted by z and the radial coordinate, which is taken along the solid-liquid interface by r, we have

$$\frac{1}{r}\frac{\partial}{\partial r}\left(r\frac{\partial T}{\partial r}\right)+\frac{\partial^2 T}{\partial z^2}=0, \tag{1}$$

$$\frac{1}{r}\frac{\partial}{\partial r}\left(r\frac{\partial T_p}{\partial r}\right)+\frac{\partial^2 T_p}{\partial z^2}=0, \tag{2}$$

where T and T_p denote the temperature in the liquid phase and in the particle, respectively.

At the particle-liquid boundary, $[z-(a+h_\infty)]^2+r^2=a^2$, the continuity of the temperature and of the heat flux yields

$$T=T_p, \quad \boldsymbol{\nabla}(k_l T-k_p T_p)\cdot\mathbf{n}=0, \tag{3}$$

where $\mathbf{n}$ denotes the normal to the particle-melt boundary that is pointing into the liquid and $\boldsymbol{\nabla}$ is the gradient vector. If we neglect the kinetic and hydrodynamic effects, the solid-liquid interface equilibrium temperature is given by [5]

$$T_{\rm int}=T_m+\Delta T_{\rm curv}, \tag{4}$$

where $\Delta T_{\rm curv}$ is the curvature undercooling given by the Gibbs-Thomson formula

$$\Delta T_{\rm curv}=-\frac{\sigma_{\rm sl} T_m}{L}\mathcal{K}, \tag{5}$$

and where $\mathcal{K}$ is the curvature of the interface (positive when the center of curvature lies in the solid phase) and $\sigma_{\rm sl}$ is the surface energy. Far away from the interface, the temperature gradient in the liquid phase is maintained at G,

$$\frac{\partial T}{\partial z}=G, \quad \text{as} \quad z\to\infty. \tag{6}$$

III. INTERFACE PROFILE

On the understanding that (i) the particle is small compared to the horizontal extent of the solid-liquid interface, (ii) the particle is placed in the near proximity of the front, and (iii) the solid-liquid interface is deformable, we have from Eqs. (1)–(6),

$$T(r,z)=T_m+Gz-Ga^3\left(\frac{\alpha-1}{2+\alpha}\right)\frac{z-(h_\infty+a)}{[\{z-(h_\infty+a)\}^2+r^2]^{3/2}}, \tag{7}$$

where $\alpha=k_p/k_l$ is the ratio of the particle's thermal conductivity to that of the melt. This solution assumes that the interface is deformable. For a nondeformable interface, the method of images must be used to find $T(r,z)$ that takes the value T_m at $z=0$. The interface temperature is thus found by evaluating Eq. (7) at $z=0$. We have

$$T_{\rm int}(r)=T_m+a^3G\left(\frac{\alpha-1}{\alpha+2}\right)\frac{(h_\infty+a)}{[(h_\infty+a)^2+r^2]^{3/2}}. \tag{8}$$

The interface curvature is, then, obtained from Eq. (4),

$$\mathcal{K}=-\frac{LGa^3}{T_m\sigma_{\rm sl}}\left(\frac{\alpha-1}{2+\alpha}\right)\frac{h_\infty+a}{[(h_\infty+a)^2+r^2]^{3/2}}. \tag{9}$$

The front's curvature is expressed in terms of the interface profile $h(r)$ as

$$\mathcal{K}=-\frac{h''(r)}{[1+(h')^2]^{3/2}}-\frac{h'(r)}{r[1+(h')^2]^{1/2}}, \tag{10}$$

where the prime notation stands for derivative with respect to r. On equating Eqs. (9) and (10) we obtain the following system of two first-order differential equations for the profile $h(r)$,

$$\frac{dh}{dr}=v$$

$$\frac{dv}{dr}=-\frac{v}{r}(1+v^2)+\frac{LGa^3}{T_m\sigma_{\rm sl}}\left(\frac{\alpha-1}{\alpha+2}\right)\times(1+v^2)^{3/2}\frac{h_\infty+a}{[(h_\infty+a)^2+r^2]^{3/2}}. \tag{11}$$

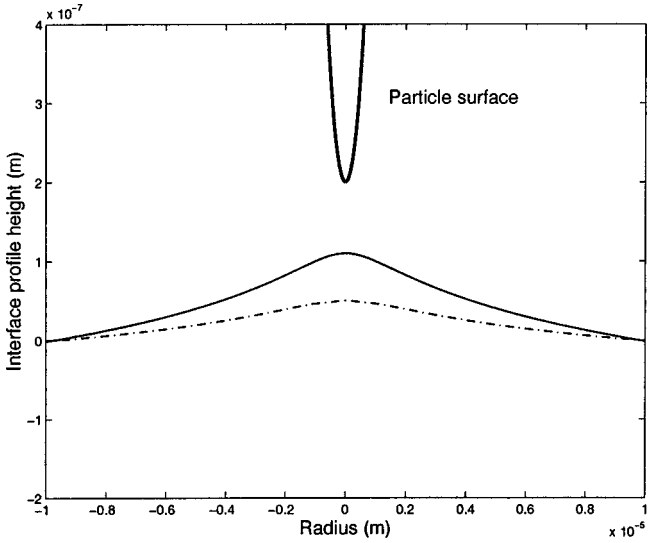

FIG. 2. Plot of the interface profile $h(r)$ versus the radius r (to the left of the origin, the tick marks are shown at $-r$ along the axis) for two values of α, namely, $\alpha=0$ (continuous line) and $\alpha=0.35$ (the dashdotted line). The particle's radius is $a=1.0\times10^{-6}$ m and $h_\infty=0.2a$. The particle's surface is shown above the interface profile. In order to depict the interface deformation, the vertical scale is chosen much smaller than the horizontal scale, thus the nonspherical look of the particle's surface.

The above system of equations is complemented by a symmetry condition at the origin, namely $h'(0)=0$, and a boundedness condition at infinity, namely, $h(r)\rightarrow0$ as $r\rightarrow\infty$. The latter is due to the fact that far away from the particle, the interface location remains undisturbed at $z=0$, so Eq. (11) is a boundary value problem for $h(r)$. The system of equations is solved numerically as an initial-value problem by using the symmetry condition and an assumed value for $h(r)$ at $r=0$. The correct value of $h(0)$ (within discretization error) is the one that will cause the profile $h(r)$ to approach zero as r becomes large. In our numerical experiments, we have (arbitrarily) used the condition $h=0$ at r equal to five particle diameters. The calculation of $h(0)$ can be made more precise by imposing that $h=0$ at a larger distance from the origin.

We consider the numerical solution of Eq. (11) for a particle of radius $a=10^{-6}$ m, latent heat of fusion per unit volume $L=4.6\times10^{7}$ J/m^3, $T_m=328$ K, and $\sigma_{sl}=0.03$ J/m^2. We have investigated first the influence of the thermal conductivity ratio α on the interface morphology. We fixed the thermal gradient $G=30\,800$ K/m and considered, first, two values for α that are less than unity, namely, $\alpha=0$ (perfectly insulating particle) and $\alpha=0.35$ (typical value for succinonitrile with polystyrene particles). Figure 2 depicts the profiles for these cases. We observe that $\alpha=0$ is associated with the largest distortion in the profile; and as α increases toward 1, the curvature of the interface decreases until it reaches zero at $\alpha=1$. The gap thickness at $r=0$ is given by $g_0=h_\infty-h_i$. We find $g_0=9\times10^{-8}$ m for $\alpha=0$ and $g_0=1.5\times10^{-7}$ m for $\alpha=0.35$. Figure 3 depicts a plot of the interface profile for a thermal conductivity ratio α greater than unity. Two values of α are selected, namely, $\alpha=381$

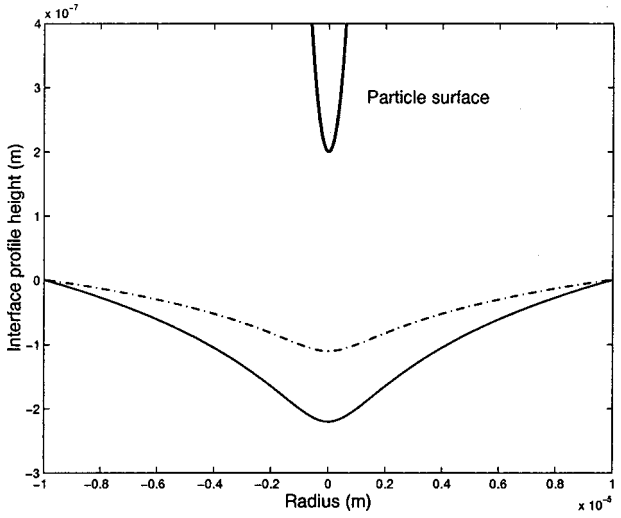

FIG. 3. Plot of $h(r)$ versus r for $G=30\,800$ K/m and for $\alpha=4$ (dashdotted line) and $\alpha=381$ (continuous line); $a=10^{-6}$ m and $h_\infty=0.2a$.

(typical value for succinonitrile containing SiC particles) and $\alpha=4$ (for comparison purposes). The largest interface deformation is achieved with the largest α value. The gap thickness at the origin is found to be $g_0=4.2\times10^{-7}$ m and $g_0=3.1\times10^{-7}$ m for $\alpha=381$ and $\alpha=4$, respectively.

The influence of the imposed thermal gradient on the morphology of the solid-liquid interface is shown in Figs. 4 and 5. In Fig. 4, we have fixed the value of $\alpha=0.35$ and considered two values for G, namely, $G=30\,800$ and $10\,800$ K/m. The largest deviation from the planar interface is attained for the larger thermal gradient. The gap separation is found to be $g_0=1.5\times10^{-7}$ and 1.8×10^{-7} m for $G=30\,800$ and $10\,800$ K/m, respectively. For $\alpha>1$, however, the thermal effect has the opposite effect, i.e., while the larg-

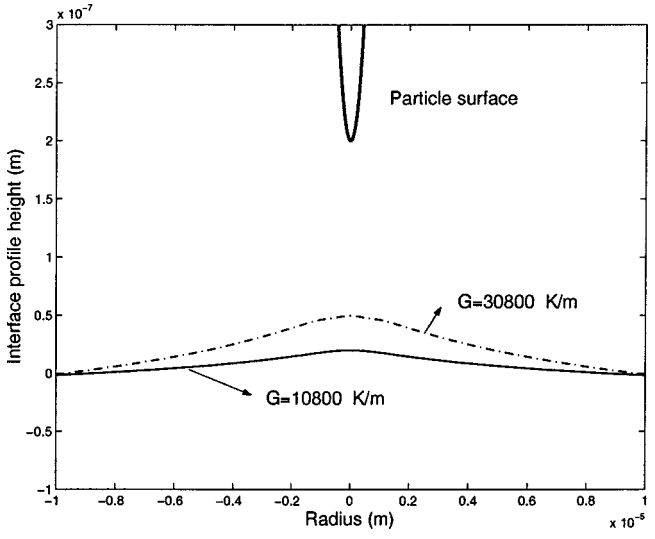

FIG. 4. Plot of the interface profile $h(r)$ versus r for $\alpha=0.35$ and two values of the thermal gradient G, $G=10\,800$ (continuous line) and $30\,800$ K/m (dash-dotted line); $a=10^{-6}$ m and $h_\infty=0.2a$. The gap separation at the origin is 1.5×10^{-7} and 1.8×10^{-7} m for $G=30\,800$ and $10\,800$ K/m, respectively.

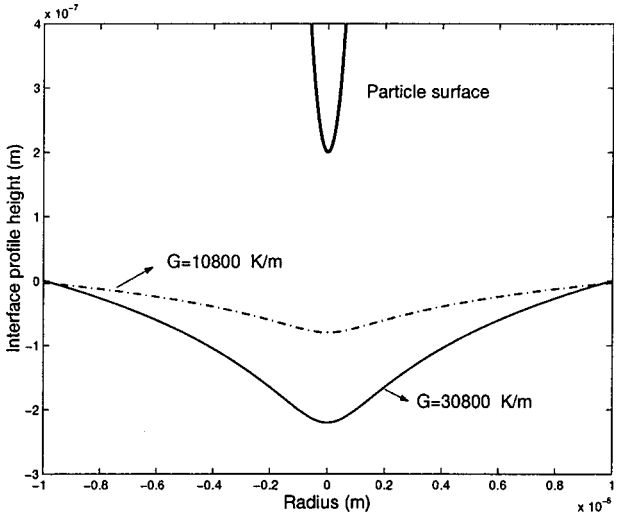

FIG. 5. Interface profile $h(r)$ versus r for $\alpha=381$ and two values of the thermal gradient G, $G=10\,800$ (dash-dotted line) and 30 800 K/m (continuous line); $a=10^{-6}$ m and $h_\infty=0.2a$. The gap separation at the origin are 4.2×10^{-7} and 2.8×10^{-7} m for $G=10\,800$ and 30 800 K/m, respectively.

est deviation from the horizontal profile is achieved at the larger value of G, an increase in G leads to an increase in the gap separation between the interface and the particle's surface.

IV. THERMAL FORCE

In the previous section, we have analyzed the interface deformation induced by the difference in thermal conductivities between the particle and the melt. The change in the front curvature gives rise to a pressure change $\mathcal{P}_{\rm th}=\sigma_{\rm sl}\mathcal{K}$, and upon using Eq. (9), we have

$$\mathcal{P}_{\rm th}=\frac{LGa^3(1-\alpha)(h_\infty+a)}{(2+\alpha)T_m[(h_\infty+a)^2+r^2]^{3/2}}. \tag{12}$$

This pressure change, in turn, gives rise to a force $F_{\rm th}$ given by

$$F_{\rm th}=\int_0^\infty 2\pi r\mathcal{P}_{\rm th}dr. \tag{13}$$

The evaluation of the above equation gives

$$F_{\rm th}=\frac{2\pi LGa^3(1-\alpha)}{(2+\alpha)T_m}. \tag{14}$$

The dependence of $F_{\rm th}$ on α is such that the force is attractive (toward the front) for $\alpha>1$ and repulsive for $\alpha<1$. Note that the magnitude of the thermal force $F_{\rm th}$ increases as α decreases if $0\leqslant\alpha<1$, and increases as α increases if $\alpha>1$; so a perfectly insulating particle yields the largest repulsive force while an infinitely conducting particle yields the largest attractive force. Thus, the thermal force acts in such a way as to increase the critical growth rate as $\alpha\to0$, and to decrease the critical growth rate as $\alpha\to\infty$. These findings are in agreement with the remarks made by Chernov and Temkin (Ref. [5], p. 34). Note also that the magnitude of the thermal force is proportional to the factor $(1-\alpha)/(2+\alpha)$ whose values lie between -1 and $\frac{1}{2}$ for $0\leqslant\alpha<\infty$. Thus the strength of $F_{\rm th}$ is not strongly affected by the value of α.

TABLE I. Estimates for the drag force $F_{\rm drag}$ (for two values of the growth rate V), the disjoining pressure force $F_{\rm DP}$ and the thermal force $F_{\rm th}$ for the case of succinonitrile containing SiC particles of radius (top) $a=10^{-5}$ m and (bottom) $a=50\times10^{-6}$ m; g_0 is the gap width at the origin

g_0 (m)	$F_{\rm drag}$ (N)	$F_{\rm drag}$ (N)	$F_{\rm DP}$ (N)	$F_{\rm th}$ (N)
	$V=10^{-4}$ m/s	$V=10^{-1}$ m/s		
		$a=10^{-5}$ m		
10^{-5}	4.9×10^{-11}	4.9×10^{-8}	1.7×10^{-15}	9.4×10^{-6}
10^{-6}	4.9×10^{-10}	4.9×10^{-7}	1.7×10^{-13}	9.4×10^{-6}
10^{-7}	4.9×10^{-9}	4.9×10^{-5}	1.7×10^{-9}	9.4×10^{-6}
		$a=50\times10^{-6}$ m		
10^{-5}	1.2×10^{-9}	1.2×10^{-6}	8.3×10^{-15}	1.2×10^{-3}
10^{-6}	1.2×10^{-8}	1.2×10^{-5}	8.3×10^{-13}	1.2×10^{-3}
10^{-7}	1.9×10^{-7}	1.2×10^{-4}	8.3×10^{-11}	1.2×10^{-3}

Let us compare the thermal force $F_{\rm th}$, Eq. (14), to other forces that act on the particle. In a microgravity environment, it is generally recognized that the outcome of the interaction between a particle and a solid-liquid interface depends primarily on the competition between two forces: a drag force $F_{\rm drag}$ [19] that resists the motion and thus pushes the particle against the interface, and a repulsive force $F_{\rm DP}$ [20] that arises as a result of the action of the disjoining pressure in the melt film separating the particle from the solid front. These forces depend on both the gap width and the particle's radius while the drag force depends also on the growth velocity. As in Ref. [5] to obtain rough estimates for these forces, we approximate the gap profile by its value at the origin. We have

$$F_{\rm drag}\approx\frac{6\pi\mu a^2V}{g_0},\quad F_{\rm DP}\approx\frac{a\mathcal{A}}{6g_0^2}, \tag{15}$$

where μ is the melt's dynamic viscosity, V the growth rate of the interface, $\mathcal{A}$ the Hamaker constant, and g_0 is the gap width at $r=0$.

For comparison purposes, we consider an experimental setup consisting of succinonitrile containing SiC particles. The values of the physical constants are taken from Ref. [15], namely, $\mu=2.6\times10^{-3}$ kg/m s, $\alpha=381$, $G=10\,800$ K/m, $L=4.6\times10^{7}$ J/m^{-3}, and $T_m=328$ K. We consider a Hamaker constant $\mathcal{A}=10^{-19}$ J and particles with radii $a=10^{-5}$ and 5×10^{-5} m. We consider two values for the growth rate, namely, $V=10^{-4}$ and 10^{-1} m/s. We obtain the following values (Table I) for the drag force $F_{\rm drag}$, the disjoining pressure force $F_{\rm DP}$, and the thermal force $F_{\rm th}$ for three representative values of the gap thickness g_0. The displayed values are only order of magnitude estimates, but they give insight on the importance of the thermal force.

These estimates indicate that for an SiC particle of radius 10^{-5} m, F_{th} is greater in magnitude than the drag force for V as high as $1.5\times10^{-1}\,\mathrm{m\,s^{-1}}$; and the balance between the thermal force and the disjoining pressure force requires a gap thickness $g_0\approx4\times10^{-9}$ m. This interlayer thickness is comparable to molecular dimensions. Thus, these rough estimates demonstrate the significance of the thermal force. In this particular case, the thermal force seems to be the main force determining the behavior of the particle at the solid-liquid interface.

The above analysis has shown that two scenarios stand out. First, in the case $\alpha>1$, such as in the SCN-SiC system, both F_{th} and F_{drag} are attractive. Therefore, both contribute in pushing the particle against the interface and the determination of the interface growth rate, when the forces are at equilibrium, requires balancing F_{DP} with F_{drag} and F_{th} together and not F_{drag} alone. The equilibrium of the forces, i.e., $F_{DP}=F_{drag}+F_{th}$ implies

$$V=\frac{g_0}{6\pi\mu a^2}(F_{DP}-F_{th}). \tag{16}$$

Thus, the inclusion of the thermal force seems to imply a decrease in the equilibrium growth rate. In the case $\alpha<1$, such as in the SCN-PS experimental system, F_{th} is repulsive. If the magnitude of F_{th} is greater than that of F_{drag}, the particle stays ahead of the moving interface and the disjoining pressure may never enter into play. However, if F_{th} has a magnitude that is smaller than that of F_{drag}, then the outcome of the interaction will be determined from a balance between the disjoining pressure force and the difference between F_{drag} and F_{th}, i.e., $F_{drag}-F_{th}$. The equilibrium condition implies

$$V=\frac{g_0}{6\pi\mu a^2}(F_{DP}+F_{th}). \tag{17}$$

In this case, the inclusion of the thermal force yields a higher equilibrium growth rate.

V. COMPARISON WITH EXPERIMENT

Numerous experiments have been carried out for the purpose of elucidating the particle-interface phenomenon. Very few, however, deal with the interaction of particles with a planar interface in a microgravity environment so that comparison with the predictions of the present theory can be performed. The experiments of Zubko, Lobanov, and Nikonova [11] and Schevezov and Weinburg [21] may be the only two we are able to find that can provide a suitable illustration of the thermal force put forth in this paper. In their investigation of the influence of the thermal conductivities of the particle and the melt on the capture of particles by crystals, Zubko, Lobanov, and Nikonova [11] examined the solidification, by the Bridgman method, of three different materials, namely, bismuth, tin, and zinc that have been mixed with particles of different materials such as tungsten, iron, molybdenum, nickel, chromium, or tantalum. The solid-liquid interface remained planar throughout the range of steady state growths considered in the experiment. A microscope was utilized to detect the behavior of the particles at the crystallization front. The experiments showed that the nature of the interaction between the particles and the crystallization front depends primarily on the ratio of the thermal conductivities of the particle and the melt, i.e., if $\alpha>1$ the particle is captured and if $\alpha<1$ it is rejected regardless of the wetting properties of the particles. These experimental findings are in agreement with our predictions using the thermal force. Also, a part of the experimental work of Schevezov and Weinburg [21] deals with the interaction of iron particles with a moving and planar solid-liquid interface in lead and lead alloy. They observed no evidence of particle rejection for growth rates up to 30 μm/sec and for particles of various sizes. This observation contradicts other theories, which stated that small particles are rejected by the interface. This observation may be explained in terms of the thermal force, since for a system consisting of lead with iron particles $\alpha>1$, the thermal force is attractive and thus pushes the particles against the front.

VI. CONCLUDING REMARKS

Many theoretical studies have attempted to explain how the thermal conductivity of the particle affects its behavior as it is intercepted by an advancing solid-liquid interface. Most of these studies have adopted the following approach: the thermal conductivity contrast, being a cause of the interfacial distortion, makes the gap separation depend on the thermal properties of the particle and the melt. The gap width is approximated and the result incorporated into the formula for the drag force, Eq. (15). Finally, a modified expression for the drag force, which now depends on the coefficients of thermal conductivities of the particle and the melt, is derived and used in the overall force balance to calculate the critical velocity for particle capture. Other studies have simply considered *ad hoc* expressions for the drag force that also include the thermal conductivities of the particle and the melt. These approaches are incorrect because they yield expressions for the hydrodynamic drag force that depend on the thermal properties of the particles and thus make no sense physically. For instance, modified formulas for the drag force have been derived, which show that the force vanishes when the particle is perfectly insulating. We refer the reader to the recent papers by Kaptay [22] and [23] and to references therein for a thorough discussion of results obtained using this approach.

In this paper, we have brought to light an expression for the thermal force that is induced by the front's curvature due to the thermal conductivity difference [Eq. (14)]. Given that α differs from unity in any experimental system and given its significant magnitude, the thermal force is an important factor in any particle-interface interaction study. The calculation of the critical velocity must account for three separate forces, namely, the hydrodynamic drag force that is independent of the thermal properties of the melt and particle, the disjoining pressure force, and the thermal force, Eq. (14).

We have also investigated the thermal effects induced by the presence of a nondeformable particle on the shape of the

solid-liquid interface. We have made the usual assumption that the interface growth rate is low enough that the interface can be considered immobile when calculating the thermal field. This immobile interface assumption is a standard approximation in theoretical works that incorporate the thermal effects in the analysis [4–18]. Results were obtained for a succinonitrile with polystyrene particles (SCN-PS) ($\alpha = 0.35$) and for succinonitrile with SiC particles (SCN-SiC) ($\alpha = 381$). We have found that for a SCN-PS system, the curvature of the interface profile is positive, i.e., the solid phase bulges into the liquid phase behind the particle in agreement with previous studies. An increase in the thermal gradient increases the front's curvature and reduces the gap separation between the interface and the particle at the origin. For an SCN-SiC system, the curvature of the interface profile is found to be negative. An increase in the thermal gradient is associated with an increase in the front's curvature and an increase in the gap separation.

ACKNOWLEDGMENT

This work was supported by a grant from the National Science Foundation (Grant No. DMS-9700380).

[1] A. Endo, H. S. Chauhan, T. Egi, and Y. Shiohara, J. Mater. Sci. **11**, 795 (1996).
[2] K. A. Jackson and B. Chalmers, J. Appl. Phys. **29**, 1178 (1958).
[3] C. Korber, G. Rau, M. D. Cosman, and E. G. Cravalho, J. Cryst. Growth **72**, 649 (1985).
[4] D. Shangguan, S. Ahuja, and D. M. Stefanescu, Metall. Trans. A **23**, 669 (1992).
[5] A. A. Chernov and D. E. Temkin, in *Current Topics in Materials Science*, edited by E. Kaldis and H. J. Scheel (North-Holland, Amsterdam, 1977), Vol. 2, pp. 3–77.
[6] P. K. Rohatgi, R. Asthana and S. Das, Int. Metall. Rev. **31**, 115 (1988).
[7] D. Li and A. W. Neumann, in *Applied Surface Thermodynamics*, edited by A. W. Neumann and J. K. Spelt (Dekker, New York, 1996), Vol. 63, pp. 557–629.
[8] A. A. Chernov, D. E. Temkin, and A. M. Mel'nikova, Sov. Phys. Crystallogr. **22**, 656 (1977).
[9] J. Pötschke and V. Rogge, J. Cryst. Growth **94**, 726 (1989).
[10] J. K. Kim and P. K. Rohatgi, Metall. Mater. Trans. A **29**, 351 (1998).
[11] A. M. Zubko, V. G. Lobanov, and V. V. Nikonova, Sov. Phys. Crystallogr. **18**, 239 (1973).
[12] D. M. Stefanescu, B. K. Dhindaw, S. A. Kacar, and A. Moitra, Metall. Trans. A **19A**, 2847 (1988).
[13] H. Pang, D. M. Stefanescu, and B. K. Dhindaw, in *The Second International Conference on Cast Metal Matrix Composites, Tuscaloosa, AL, 1993*, edited by D. M. Stefanescu and S. Sen (American Foundrymen's Society, DesPlaines, IL, 1994), pp. 57–69.
[14] S. Ahuja, D. M. Stefanescu, and B. K. Dhindaw, in *The Second International Conference on Cast Metal Matrix Composites, Tuscaloosa, AL* (Ref. [13]), pp. 44–56.
[15] D. M. Stefanescu, R. V. Phalnikar, H. Pang, S. Ahuja, and B. K. Dhindaw, ISIJ Int. **35**, 700 (1995).
[16] R. Sasikumar, T. R. Ramamohan, and B. C. Pai, Acta Metall. **37**, 2085 (1989).
[17] P. Casses and M. A. Azouni, J. Cryst. Growth **130**, 13 (1993).
[18] R. Sasikumar and T. R. Ramamohan, Acta Metall. Mater. **39**, 517 (1991).
[19] H. Brenner, Chem. Eng. Sci. **16**, 242 (1961).
[20] E. J. Verwey and J. Th. G. Overbeek, *The Theory and Stability of Lyophobic Colloids* (Elsevier, New York, 1948), Vol. 18, pp. 239–241.
[21] C. E. Schevesov and F. Weinburg, Metall. Trans. B **16B**, 367 (1985).
[22] G. Kaptay, Metall. Trans. A **31A**, 1695 (2000).
[23] G. Kaptay, Metall. Mater. Trans. A **32A**, 993 (2001).